Title
An acidic motif retains vesicular monoamine transporter 2 on large dense core vesicles.

Journal
The Journal of cell biology, 152(6)

ISSN
0021-9525

Authors
Waites, CL
Mehta, A
Tan, PK
et al.

Publication Date
2001-03-01

DOI
10.1083/jcb.152.6.1159

Peer reviewed

An Acidic Motif Retains Vesicular Monoamine Transporter 2 on Large Dense Core Vesicles

Clarissa L. Waites,* Anand Mehta,* Philip K. Tan,* Gary Thomas,‡ Robert H. Edwards,* and David E. Krantz*

*Graduate Programs in Neuroscience and Cell Biology, Departments of Neurology and Physiology, University of California, San Francisco School of Medicine, San Francisco, California 94143-0435; and ‡Vollum Institute, Oregon Health Sciences University, Portland, Oregon 97201

Abstract. The release of biogenic amines from large dense core vesicles (LDCVs) depends on localization of the vesicular monoamine transporter VMAT2 to LDCVs. We now find that a cluster of acidic residues including two serines phosphorylated by casein kinase 2 is required for the localization of VMAT2 to LDCVs. Deletion of the acidic cluster promotes the removal of VMAT2 from LDCVs during their maturation. The motif thus acts as a signal for retention on LDCVs. In addition, replacement of the serines by glutamate to mimic phosphorylation promotes the removal of VMAT2 from LDCVs, whereas replacement by alanine to prevent phosphorylation decreases removal. Phosphorylation of the acidic cluster thus appears to reduce the localization of VMAT2 to LDCVs by inactivating a retention mechanism.

Key words: acidic cluster • large dense core vesicles • phosphorylation • VMAT2 • furin

Introduction

Neurotransmitter release involves the regulated exocytosis of multiple, distinct types of secretory vesicle including synaptic vesicles (SVs)[1] and large dense core vesicles (LDCVs). Although SVs and LDCVs both undergo regulated exocytosis, they differ in the site and mode of release, as well as in their contents. SVs cluster at the nerve terminal, mediate the rapid release of neurotransmitter into the synaptic cleft, and store classical neurotransmitter (Sudhof, 1995; Calakos and Scheller, 1996). In contrast, LDCVs appear in dendrites as well as axons, release their contents more slowly and in response to different stimuli than SVs, and contain neuromodulatory peptides, growth factors, and certain classical transmitters such as monoamines (De Camilli and Jahn, 1990; Martin, 1994). SVs and LDCVs also differ in their biogenesis. SVs form locally at the nerve terminal, whereas LDCVs bud directly from the trans-Golgi network (Kelly and Grote, 1993; Tooze et al., 1993). Differences in protein sorting at these sites presumably underlie the differences in protein composition and hence vesicle function. However, little is known about the cellular mechanisms that target proteins to different classes of neurosecretory vesicles. To identify the signals that target proteins to SVs and LDCVs, we have focused on a family of membrane proteins required for the exocytotic release of neurotransmitter.

Classical transmitters are synthesized in the cytoplasm and require packaging into secretory vesicles by specific transport proteins. The localization of these proteins to SVs, LDCVs, or other types of neurosecretory vesicle determines the site of neurotransmitter storage and hence the mode of release. Dopamine in particular undergoes release from the cell body and dendrites of midbrain dopamine neurons as well as from nerve terminals in the striatum (Geffen et al., 1976; Cheramy et al., 1981; Robertson et al., 1991; Heeringa and Abercrombie, 1995; Jaffe et al., 1998), and somatodendritic release has been proposed to regulate neuronal activity (Aghajanian and Bunney, 1974; Grace and Bunney, 1995). Consistent with the release of dopamine at these sites, the vesicular monoamine transporter (VMAT2) responsible for dopamine transport into secretory vesicles resides on LDCVs and tubulovesicular structures in the cell body and dendrites as well as on SVs at the nerve terminal (Weihe et al., 1994; Nirenberg et al., 1995, 1996, 1997; Peter et al., 1995). Studies of leech Retzius neu-

Address correspondence to R.H. Edwards, Graduate Programs in Neuroscience and Cell Biology, Departments of Neurology and Physiology, UCSF School of Medicine, 513 Parnassus Ave., San Francisco, CA 94143-0435. Tel.: (415) 502-5687. Fax: (415) 502-5687. E-mail: edwards@itsa.ucsf.edu

Dr. Krantz's current address is Department of Psychiatry and Biobehavioral Sciences, UCLA School of Medicine, Los Angeles, CA 90095.

[1]*Abbreviations used in this paper:* BFA, brefeldin A; GST, glutathione-S-transferase; HA, hemagglutinin; LDCV, large dense core vesicle; PNS, post-nuclear supernatant; SgII, secretogranin II; SLMV, synaptic-like microvesicle; SV, synaptic vesicle.

rons further support the release of serotonin from both LDCVs located in the cell body and terminal and from SVs restricted to the terminal (Bruns and Jahn, 1995). Since the localization of VMAT2 to LDCVs influences the site and mode of monoamine release, the expression of VMAT2 on LDCVs presumably contributes to the role of dopamine, norepinephrine, and serotonin in neuromodulation.

As an integral membrane protein, VMAT2 must also contain signals that direct its trafficking to LDCVs (Krantz et al., 2000). To identify the signals responsible for the membrane trafficking of VMAT2, we have used heterologous expression in PC12 cells, where VMAT2 targets preferentially to LDCVs (Liu et al., 1994; Varoqui and Erickson, 1998; Krantz et al., 2000). We previously identified a dileucine-like motif in the cytoplasmic COOH terminus of VMAT2 that mediates internalization from the plasma membrane (Tan et al., 1998). The closely related vesicular acetylcholine transporter (VAChT) contains a very similar motif, but unlike VMAT2, VAChT targets preferentially to synaptic-like microvesicles (SLMVs) rather than LDCVs in PC12 cells (Liu and Edwards, 1997; Varoqui and Erickson, 1998). VMAT2 also differs from VAChT 4 and 5 residues upstream of the dileucine-like signal, positions shown to be important for the trafficking of other proteins (Pond et al., 1995; Dietrich et al., 1997). Although these residues do not affect the endocytosis of either VMAT2 or VAChT (Tan et al., 1998), we have recently found that they influence targeting to LDCVs and account in part for the observed differences in steady state localization between these two transport proteins (Krantz et al., 2000).

The analysis of COOH-terminal deletions in VMAT2 now implicates an acidic motif containing two serines phosphorylated by casein kinase 2 (CK2; Krantz et al., 1997) in targeting to LDCVs. After budding from the TGN, LDCVs undergo a maturation process in which proteins destined for other compartments such as lysosomes are removed (Tooze et al., 1993; Kuliawat et al., 1997; Klumperman et al., 1998). Deletion of the COOH-terminal acidic motif reduces the expression of VMAT2 on LDCVs by promoting its removal during LDCV maturation. The motif thus appears to act as a signal for retention on LDCVs. Interestingly, the TGN endoprotease furin contains a similar acidic cluster with two serines phosphorylated by CK2. Phosphorylation of this motif increases furin retrieval from LDCVs (Jones et al., 1995; Dittie et al., 1997), apparently through an interaction with the novel cytosolic adaptor protein PACS-1 (phosphofurin acidic cluster sorting protein 1) (Wan et al., 1998). In VMAT2, replacement of serines in the acidic motif by aspartate to mimic phosphorylation also promotes the removal of VMAT2 during LDCV maturation, whereas replacement by alanine to prevent phosphorylation increases localization to LDCVs. Phosphorylation thus appears to promote VMAT2 retrieval from immature LDCVs by blocking the role of the acidic motif in retention. Very similar to furin, the phosphorylated form of the acidic cluster in VMAT2 also binds to PACS-1. Despite the similarities between VMAT2 and furin, however, VMAT2 normally resides in LDCVs, whereas furin localizes to the TGN (Liu and Edwards, 1997; Krantz et al., 2000). Differences in phosphorylation state presumably account for the divergent steady state location of these proteins by influencing their removal from LDCVs.

Materials and Methods

Antibodies

Mouse monoclonal HA.11 antibody was obtained from Covance, the rat monoclonal hemagglutinin (HA) antibody from Boehringer, the rabbit polyclonal antiserum to secretogranin II from BioDesign, the mouse monoclonal antibody to the transferrin receptor from Zymed, the rabbit polyclonal antiserum to rab5 from Quality Controlled Biochemicals, the mouse monoclonal antibody to γ-adaptin from Transduction Laboratories, the rabbit polyclonal antibody to synaptophysin from Zymed, and the mouse monoclonal anti–his and goat polyclonal anti–glutathione-S-transferase (GST) antibodies from Amersham Pharmacia Biotech. Secondary antibodies conjugated to FITC, Texas red, Cy3, and Cy5 were obtained from Jackson ImmunoResearch Laboratories, and secondary antibodies conjugated to horseradish peroxidase from Amersham Pharmacia Biotech (anti–rabbit and anti–mouse) or Sigma-Aldrich (anti–goat). Brefeldin A was obtained from Epicentre Technologies. Drs. F. Brodsky and K. Mostov (University of California at San Francisco, San Francisco, CA) generously provided antibodies to TGN-38 and mannose-6-phosphate receptor, respectively.

Mutagenesis, Cell Culture, and Immunofluorescence

Mutagenesis was performed using the Kunkel method (Kunkel et al., 1991). PC12 cells were transfected by electroporation, and independent cell clones were isolated as previously described (Krantz et al., 2000). After plating onto glass coverslips coated with poly-L-lysine and Matrigel (Becton Dickinson) and treatment with 50 ng/ml NGF for 2–3 d, the cells were immunostained as previously described (Tan et al., 1998) and visualized by confocal laser microscopy. For the experiments with brefeldin A (BFA), the cells were incubated with 5 μg/ml BFA in standard medium for 15 min at 37°C before fixation.

Density Gradient Fractionation

PC12 cells were rinsed with cmf-PBS, harvested in 0.3 M sucrose, 10 mM Hepes, pH 7.4 (sucrose-Hepes buffer) containing 2 mM Mg EGTA, 1 μg/ml leupeptin, 1 μg/ml pepstatin, and 10 μg/ml PMSF, and the cells were disrupted at a clearance of 10 μm in a ball-bearing homogenizer. After pelleting the nuclei at 1000 *g* for 8 min, the resulting post-nuclear supernatant (PNS) was layered onto a linear 0.6–1.6 M sucrose gradient and sedimented to equilibrium at 30,000 rpm for 12–16 h in an SW41 rotor at 4°C. Fractions were collected from the top.

Velocity Gradient Sedimentation

Metabolic labeling with ^{35}S-sulfate was done as done previously described (Tooze and Huttner, 1990; Dittie et al., 1996). In brief, PC12 cells were rinsed twice with sulfate-free medium, incubated at 37°C for 30 min, and then labeled for 5 min in the same medium containing 0.5 mCi/ml ^{35}S-sulfate (NEN Life Science Products). To label secretogranin II (SgII) in the TGN, the cells were chilled and harvested. To allow labeled SgII to enter iLDCVs, the labeled cells were incubated at 37°C for an additional 15 min in standard PC12 medium containing sulfate. To allow the passage of labeled SgII into mature LDCVs, cells were incubated for 6 h with 0.2 mCi/ml ^{35}S-sulfate in sulfate-free medium, and then for 12–16 h in standard PC12 medium.

Gradients were performed according to established protocols (Dittie et al., 1996; Blagoveshchenskaya et al., 1999). After labeling with ^{35}S-sulfate, cells were immediately placed on ice, rinsed with cold cmf-PBS containing 1 mM $MgSO_4$, harvested in a modified sucrose-Hepes buffer (0.25 M sucrose, 10 mM Hepes-KOH, pH 7.2) containing protease inhibitors, 1 mM EGTA, and 1 mM $MgSO_4$, the PNS prepared as above, layered onto a linear 0.3–1.2 M sucrose gradient in 10 mM Hepes-KOH, pH 7.2, and sedimented for 19 min at 25,000 rpm in an SW41 rotor at 4°C.

To separate iLDCVs from mLDCVs, fractions from the velocity gradient that contained iLDCVs or mLDCVs were identified by scintillation counting, pooled, diluted with 10 mM Hepes-KOH, pH 7.2, layered onto linear 0.9–1.7 M sucrose gradients made in 10 mM Hepes-KOH, pH 7.2, and sedimented for 21 h at 30,000 rpm in an SW41 rotor at 4°C. Fractions were collected from the top.

Western Analysis and Quantitation

Proteins were separated by electrophoresis through SDS-polyacrylamide, electroblotted to PVDF or nitrocellulose, and immunostained as previously described (Krantz et al., 2000). After detection of the bound antibodies using SuperSignal West Pico substrate (Pierce Chemical

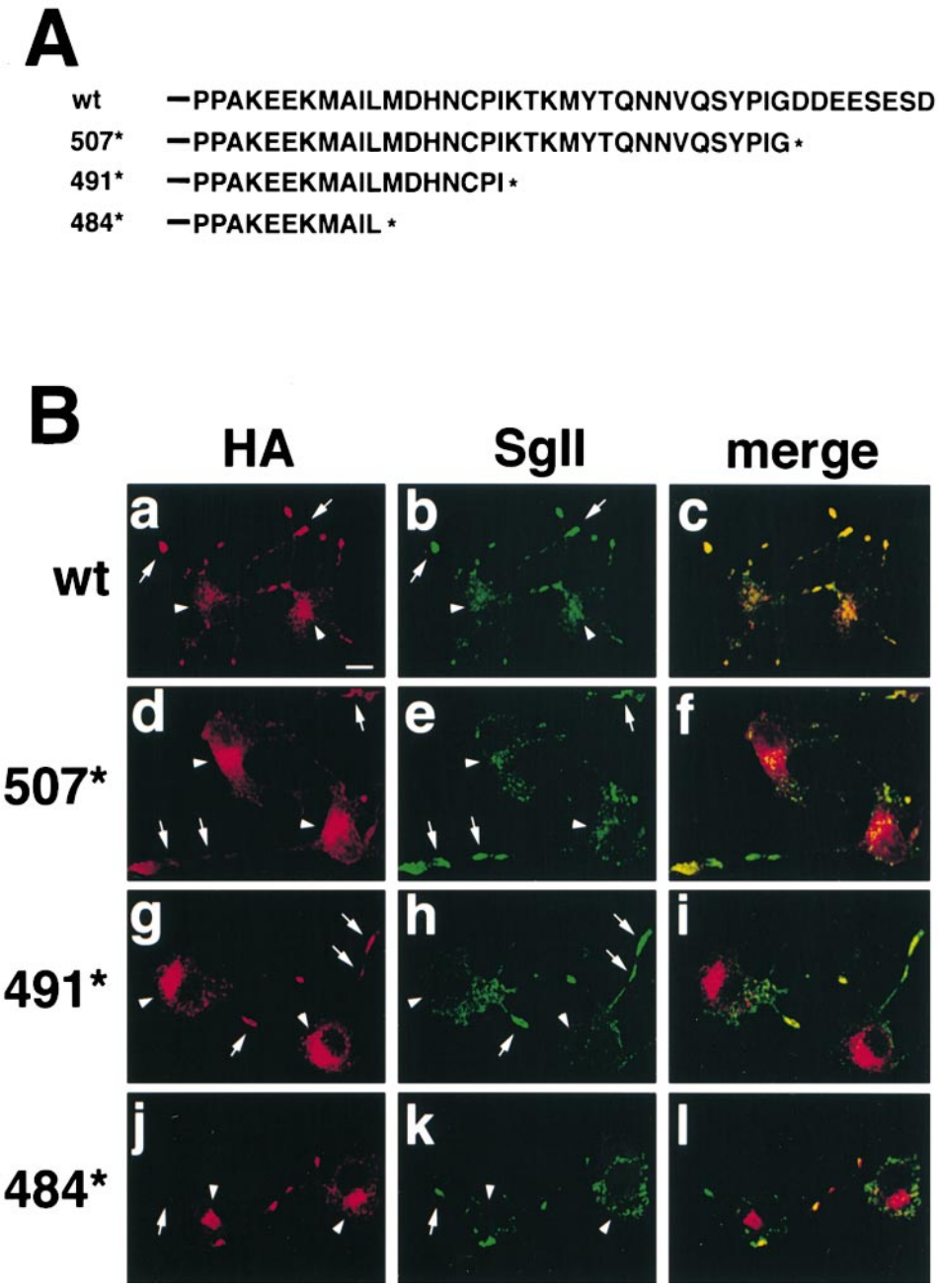

Figure 1. Analysis of COOH-terminal VMAT2 deletions by immunofluorescence. (A) Serial deletions of the VMAT2 COOH terminus were created by inserting stop codons after residues 507, 491, and 484. *The position of the inserted stop codon. (B) PC12 cells stably expressing HA-tagged wild-type VMAT2 or the deletion mutants were double stained with a mouse monoclonal antibody to HA followed by anti–mouse antibodies conjugated to Cy3 (a, d, g, and j), and with a polyclonal rabbit antiserum to SgII followed by anti–rabbit antibodies conjugated to Cy5 (b, e, h, and k), and then examined by confocal microscopy. Merged Cy3 and Cy5 images are shown in c, f, i, and l. Wild-type VMAT2 (a–c) colocalizes extensively with SgII and appears primarily at the tips of cell processes (arrows). In contrast, the mutants show little colocalization with SgII (d–l). All exhibit reduced staining at the tips of process and strong expression in the perinuclear region (arrowheads). Bar, 10 μm.

Co.), the films were optically scanned, digitized, and quantified using NIH Image.

To quantify the one-step sucrose equilibrium gradients, the amount of HA or SgII immunoreactivity in each gradient fraction was expressed as a fraction of the total HA or SgII immunoreactivity in all gradient fractions. For the two-step gradients, the sorting index for localization to i- or mLDCVs was determined by first identifying the two peak iLDCV fractions and the two peak mLDCV fractions through autoradiography for ^{35}S-sulfate–labeled SgII. The HA immunoreactivity in these peak fractions was then measured by densitometry and used to calculate the proportion of HA immunoreactivity in the two peak iLDCV fractions and the two peak mLDCV fractions relative to the total HA immunoreactivity in all four peak fractions.

Bacterial Expression and In Vitro Phosphorylation

COOH-terminal fragments of the wild-type, 507*, AA, and DD VMAT2 cDNAs were subcloned using EcoRV, inserted in-frame into the SmaI site of pGEX-3X-1 (Amersham Pharmacia Biotech), and expressed as GST fusion proteins in *Escherichia coli* as previously described (Krantz et al., 2000). The furin-binding domain of PACS-1 subcloned into pET-16b (Novagen) was also expressed and purified by Ni^{2+} chromatography. To phosphorylate the GST fusions, the proteins bound to glutathione-sepharose beads were incubated in 20 mM Tris, pH 7.5, 50 mM KCl, 1 mM DTT, and 10 mM $MgCl_2$ (phosphorylation buffer) containing 200 μM ATP, 500 μCi/μmol γ-^{32}P-ATP, and 250 U casein kinase 2 for 90 min at 30°C, washed twice in PBS with 15 mM EDTA, and tested for binding to PACS-1.

PACS-1 Binding Assay

Following a procedure described previously (Xiang et al., 2000), GST fusion proteins were bound to glutathione-sepharose beads for a final concentration of ~5 μg/ml, incubated in 150 mM NaCl, 50 mM Tris, pH 7.5, 2 mM $MgCl_2$, and 2% Triton X-100 (binding buffer) with 2.5 μg/ml purified PACS-1 for 1 h at room temperature, washed three times in binding buffer, and the proteins eluted with SDS sample buffer, separated by electrophoresis, and transferred to PVDF. Phosphorylated GST fusions were detected by autoradiography, and unlabeled GST fusions and bound PACS-1 were detected by Western analysis using anti–GST and anti–His antibodies, respectively. After autoradiography or detection of the bound antibodies by ECL Plus (Amersham Pharmacia Biotech), the films were optically scanned.

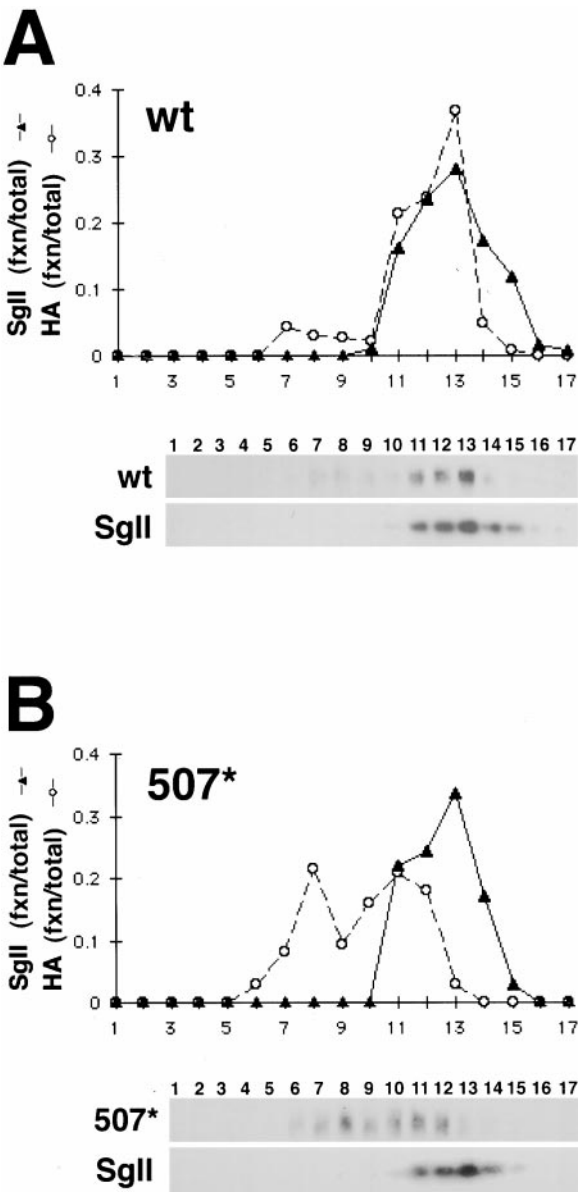

Figure 2. Density gradient fractionation of wild-type and 507* VMAT2. Post-nuclear supernatants from PC12 cells stably expressing HA-tagged wild-type (A) and 507* (B) VMAT2 were separated by equilibrium gradient centrifugation through 0.6–1.6 M sucrose. Fractions were collected and analyzed by Western blot using the monoclonal HA antibody to detect VMAT2 (A and B, top), and a polyclonal antibody to detect the LDCV marker SgII (bottom). The immunoblots were then digitized and quantified using NIH Image. For each fraction, the amount of VMAT2 and SgII is expressed as a percentage of total immunoreactivity in all the fractions. Wild-type VMAT2 cofractionates with SgII in heavy fractions, whereas 507* cofractionates to a lesser extent with SgII and appears instead in lighter fractions. The analysis of three different stable cell lines for each construct yielded similar results.

Results

Deletion of an Acidic Motif Redistributes VMAT2 Away from LDCVs

To identify signals that influence the subcellular location of VMAT2, we expressed a series of COOH-terminal truncations in PC12 cells, which produce both LDCVs and SLMVs. These constructs contain an HA epitope in the lumenal loop between transmembrane domains 1 and 2, and stop codons after residues 507, 491, and 484 (507*, 491*, and 484*; Fig. 1 A). Using immunofluorescence to compare the localization of the introduced VMAT2 with secretogranin II, a soluble protein contained in LDCVs, we found that wild-type VMAT2 colocalizes precisely with SgII at the tips of processes (Fig. 1 B, a–c). Both proteins are expressed at low levels in cell bodies. In contrast, the deletion mutants colocalize poorly with SgII (Fig. 1 B, d–l). These truncations exhibit a perinuclear staining pattern with little expression at the tips of processes, indicating the presence of a second trafficking motif at the COOH terminus of VMAT2. The distribution of 507* strongly resembles that of 491* and 484*, indicating that the last eight amino acids of VMAT2 (DDEESESD) comprise a major trafficking signal.

To confirm that deletion of the acidic cluster alters the localization of VMAT2 in PC12 cells, we analyzed the 507* mutant by density gradient fractionation. Equilibrium sedimentation through sucrose, which separates LDCVs from lighter membranes such as SLMVs and endosomes, shows that wild-type VMAT2 colocalizes with SgII in heavy, LDCV-containing fractions (Fig. 2 A), as previously observed (Krantz et al., 2000). Only very small amounts of VMAT2 appear in lighter fractions (Fig. 2 A). In contrast, the 507* mutant colocalizes less well with SgII in heavy fractions and is more prominent in lighter fractions (Fig. 2 B). Equilibrium sedimentation thus confirms the importance of a COOH-terminal acidic cluster for the localization of VMAT2 to LDCVs.

By immunofluorescence, the 507* mutant localizes to a perinuclear compartment. To identify this compartment, we used double staining to assess the colocalization of 507* with markers for various intracellular membranes. The 507* mutant does not colocalize with markers for the endoplasmic reticulum (ribophorin II), cis-Golgi (β-COP), or early endosomes (rab 5) (data not shown). The sucrose density gradient suggested expression on lighter membranes that might represent SLMVs (Fig. 2 B), but 507* shows only partial colocalization with synaptophysin (Fig. 3, a–c). The perinuclear distribution of 507* resembles that of the endosomal transferrin receptor, the late endosomal mannose 6 phosphate receptor (Fig. 3, d–i), and the lysosomal cathepsin B (data not shown). However, the merged images at higher magnification show only minor colocalization. On the other hand, 507* colocalizes more extensively with markers for the trans-Golgi network such as the clathrin adaptor protein AP-1 (data not shown) and TGN-38 (Fig. 3, j–l).

Localization of 507* to Immature LDCVs

To determine whether 507* localizes to the TGN or to closely apposed membranes, we treated the stable PC12 transformants with brefeldin A, a fungal derivative that causes fragmentation of the TGN. If expressed in the TGN, 507* should redistribute to the cell periphery after exposure to BFA. BFA indeed collapses TGN-38 as expected, but 507* remains largely perinuclear (Fig. 4 A). Since immature LDCVs (iLDCVs) bud from the TGN and may function as a specialized extension of this sorting compartment, 507* might localize instead to iLDCVs. To

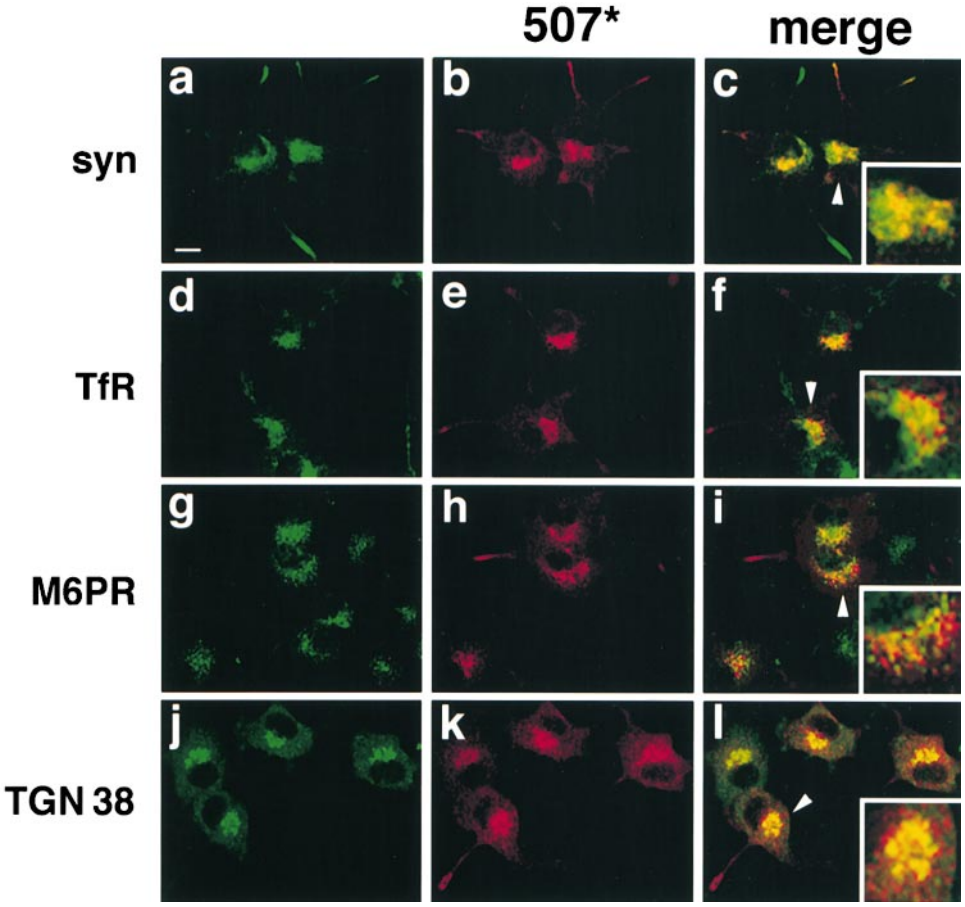

Figure 3. 507* colocalizes with TGN-38 by immunofluorescence. PC12 cells stably expressing 507* were double stained with the mouse monoclonal antibody to HA (b, h, and k) and polyclonal antibodies to synaptophysin, mannose-6-phosphate receptor (M6PR), and TGN-38 (a, g, and j), or with a rat monoclonal HA antibody (e) and a mouse monoclonal antibody to transferrin receptor (TfR) (d). Secondary antibodies conjugated to Cy3 and Cy5 were used to distinguish between 507* and the marker proteins, respectively. Merged Cy3 and Cy5 images are shown in c, f, i, and l. 507* does not colocalize with synaptophysin, TfR, or M6PR, but does colocalize extensively with TGN-38. (Insets) Perinuclear staining (arrowheads) at high magnification. Bar, 10 μm.

test this possibility, we used sulfate labeling of SgII together with gradient fractionation (Tooze and Huttner, 1990). Cells were labeled first for 5 min with ^{35}S-sulfate, which incorporates heavily into SgII as it transits the TGN, and then either chilled on ice to prevent the exit of labeled SgII from the TGN, or incubated at 37°C in medium with unlabeled sulfate for an additional 15 min to allow passage of the labeled SgII into iLDCVs. Chase for 15 min does not allow sufficient time for LDCV maturation. We then used velocity gradient fractionation to separate iLDCVs from the TGN. Autoradiography showed the shift of SgII from heavy to light fractions over the 15-min chase (Fig. 4 B), as expected. Western analysis showed that 507* colocalizes with the iLDCV-containing rather than the TGN-containing fractions (Fig. 4 B). Thus, 507* may reside on iLDCVs even though it is greatly reduced on the entire population of LDCVs (Figs. 1 and 2).

The presence of 507* on iLDCVs despite a low proportion on LDCVs raises the possibility that the mutant is removed during LDCV maturation. To determine whether 507* indeed resides on iLDCVs, we again used the labeling of SgII with ^{35}S-sulfate followed by gradient fractionation (Dittie et al., 1997; Blagoveshchenskaya et al., 1999). Labeling for 5 min followed by incubation for an additional 15 min with unlabeled sulfate allows the labeled SgII to enter iLDCVs, but not mature LDCVs. Labeling for 6 h followed by 12 h of chase allows sufficient time for the maturation of LDCVs containing labeled SgII. To separate iLDCVs from mLDCVs, and hence determine the fate of VMAT2 during LDCV maturation, we used sequential velocity and equilibrium sedimentation through sucrose. Autoradiography for ^{35}S-labeled SgII identified the fractions containing either iLDCVs or mLDCVs, and Western blotting identified those that contain VMAT2. Wild-type VMAT2 colocalizes with labeled SgII in both i- and mLDCV fractions (Fig. 5, A and B). In contrast, 507* is barely detectable in mLDCV-containing fractions, but colocalizes with labeled SgII in iLDCV-containing gradient fractions (Fig. 5, A and B). These iLDCV fractions do not contain detectable amounts of other membranes, including endosomes and SLMVs (Fig. 5 B), enabling us to distinguish between the VMAT2 on iLDCVs and on other membranes. To quantify these observations, we studied three stable cell lines each for wild-type and 507* VMAT2, and compared the amounts of protein on i- and mLDCVs. Using autoradiography to identify the peak iLDCV and mLDCV fractions, we determined the amount of VMAT2 in these fractions by densitometry and expressed the amount in either iLDCVs or mLDCVs as a fraction of total VMAT2 in all peak fractions. The analysis shows that more than half of wild-type VMAT2 in LDCVs localizes to mLDCVs, whereas only a small fraction (~10%) of 507* resides on these membranes (Fig. 5 C). In contrast, a substantially larger proportion of 507* localizes to iLDCVs relative to wild-type VMAT2. The quantitation of iLDCVs specifically excludes VMAT2 that does not cofractionate with the peak of SgII, focusing on the protein in iLDCVs rather than that in endosomes or SLMVs. A substantial proportion of the 507* that enters the regulated secretory pathway thus appears to be removed from LDCVs during maturation, indicating a role for the acidic cluster in retention on mLDCVs.

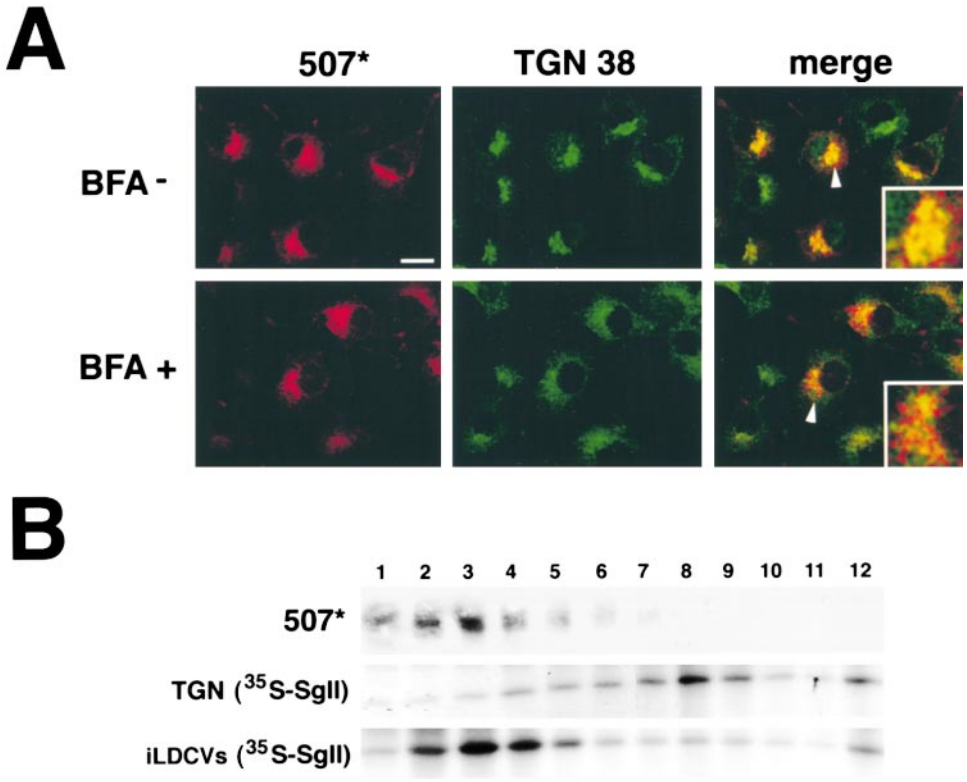

Figure 4. The 507* deletion localizes to a BFA-resistant compartment that cofractionates with iLDCVs. (A) PC12 cells stably expressing 507* were incubated without or with 5 μg/ml brefeldin A for 15 min, and then double stained with mouse monoclonal HA antibody and rabbit polyclonal TGN-38 antiserum, followed by anti–mouse antibody conjugated to Cy3 and anti–rabbit antibody conjugated to Cy5. 507* and TGN-38 colocalize in the absence but not the presence of BFA. As indicated by the dispersion of TGN-38, BFA causes fragmentation of the TGN but not the compartment containing 507*. (Insets) Perinuclear staining (arrowheads) at high magnification. Bar, 10 μm. (B) To label SgII in the TGN, cells were incubated for 5 min with 0.5 mCi/ml ^{35}S-sulfate, and then chilled on ice. To allow the labeled SgII to enter iLDCVs, cells were labeled in the same way but incubated at 37°C for an additional 15 min in medium with unlabeled sulfate before harvesting. The resulting post-nuclear supernatants were then separated by velocity sedimentation through 0.3–1.2 M sucrose, and fractions collected from the top of the gradient. Labeled SgII was detected by autoradiography and 507* protein by Western analysis using the monoclonal HA antibody. 507* comigrates with iLDCVs in fractions 2–4 rather than with the TGN in fractions 7–9.

The Role of Phosphorylation in VMAT2 Removal from Maturing LDCVs

Phosphorylation of the acidic cluster in VMAT2 may also influence targeting to LDCVs. In the case of furin, replacement of phosphorylated serines within the cluster by aspartate to mimic phosphorylation promotes retrieval from LDCVs to the TGN. In contrast, replacement of these serines by alanine to prevent phosphorylation promotes localization to LDCVs (Jones et al., 1995; Dittie et al., 1997). Since serines within the acidic cluster of VMAT2 also undergo phosphorylation by casein kinase 2 (Krantz et al., 1997), we investigated the role of phosphorylation in VMAT2 trafficking to LDCVs by replacing the serines with either alanine (AA mutant) or aspartate (DD mutant). After stable expression of the two constructs in PC12 cells, we compared their localization to SgII by immunofluorescence and density gradient fractionation. Like wild-type VMAT2, the AA mutant colocalizes extensively with SgII at the tips of neuritic processes, and appears at low levels in the cell body (Fig. 6, a–c). By gradient fractionation as well, wild-type and AA VMAT2 colocalize with SgII (Fig. 7 B). The DD mutant also colocalizes with SgII at the tips of processes and in heavy gradient fractions (Figs. 6, d–f, and 7 C), but a significant proportion does not colocalize with SgII. Rather, DD appears partially redistributed to a perinuclear compartment by immunofluorescence and to membranes lighter than LDCVs by gradient fractionation (Figs. 6, d–f, and 7 C).

Localization of the DD mutant resembles that observed for 507*, suggesting that DD may also undergo removal from LDCVs. To address this possibility, we used the two-step fractionation procedure to separate i- and mLDCVs. By this analysis, the AA mutant strongly resembles wild-type VMAT2, with more than half of the AA in the regulated secretory pathway appearing on mLDCVs (Fig. 5 C). In contrast, the localization of DD resembles that of 507*, with reduced expression on mLDCVs. Of the DD mutant sorted into LDCVs, only ~36% resides on mLDCVs (Fig. 5 C). Although the effect of the DD mutation on localization to LDCVs appears less dramatic than that of the 507* deletion, the proportion of DD on mLDCVs is clearly reduced relative to AA (~64%) and wild-type VMAT2 (~56%). Thus, phosphorylation of the acidic motif apparently influences the localization of VMAT2 to LDCVs by regulating the removal of VMAT2 during LDCV maturation.

Binding to PACS-1

The AA and DD mutations in VMAT2 have effects very similar to the analogous AA and DD mutations in furin. In both cases, replacement of the serines by aspartate to mimic phosphorylation promotes removal from iLDCVs, whereas replacement by alanine to mimic dephosphorylation promotes retention on LDCVs. However, VMAT2 normally resides on LDCVs, whereas furin normally resides in the TGN (Molloy et al., 1994; Jones et al., 1995; Schafer et al., 1995). One possible explanation for this dis-

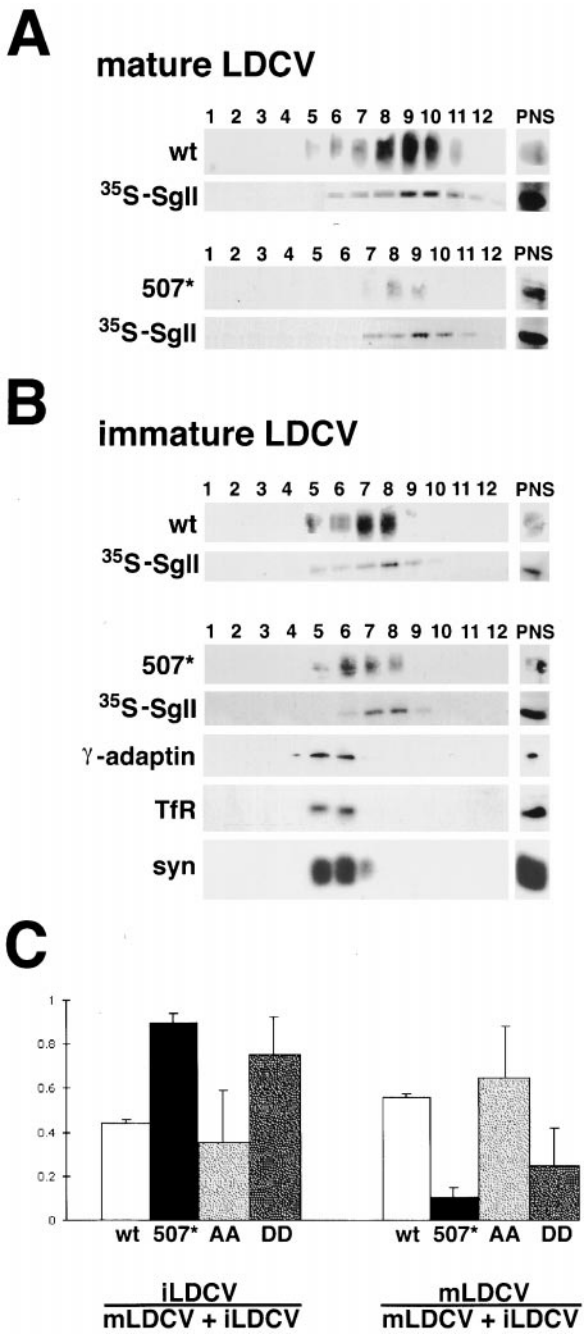

Figure 5. VMAT2 mutants 507* and DD localize preferentially to immature rather than mature LDCVs. (A) Cells were labeled with 0.2 mCi/ml ^{35}S-sulfate for 6 h, incubated for an additional 12 h with unlabeled sulfate, and PNS separated by velocity sedimentation through 0.3–1.2 M sucrose. Fractions containing mLDCVs were identified by scintillation counting, pooled, and further separated by equilibrium sedimentation through 0.9–1.7 M sucrose. The resulting fractions were collected from the top of the gradient and either submitted to autoradiography to detect radiolabeled SgII or subjected to Western analysis for HA to detect VMAT2. The starting material (PNS) is shown to the right of the fractions. Wild-type VMAT2 cofractionates with labeled SgII in mLDCVs (fractions 9 and 10) and shows enrichment in these fractions relative to the PNS. 507* cofractionates with mLDCVs in fraction 9, but is not enriched relative to the PNS. (B) Cells were labeled with 0.5 mCi/ml ^{35}S-sulfate for 5 min and incubated for an additional 15 min with unlabeled sulfate. After velocity sedimentation, the fractions containing iLDCVs were pooled and further separated by equilibrium sedimentation as described in A, followed by autoradiography for ^{35}S-sulfate, Western analysis for HA, γ-adaptin, transferrin receptor (TfR), and synaptophysin. Both wild-type and 507* VMAT2 cofractionate with labeled SgII in iLDCVs (fractions 7 and 8). Relative to the PNS, 507* is more enriched in iLDCVs than mLDCVs (A). Light membranes such as endosomes and SLMVs do not contaminate the iLDCV fractions containing ^{35}S-SgII. (C) For wt, 507*, AA, and DD VMAT2, three stable cell lines were subjected to the two-step fractionation procedure described above. Peak iLDCV and mLDCV fractions were identified by autoradiography, and the amount of VMAT2 protein in these fractions was measured using NIH Image. The amount of protein on i- and mLDCVs is expressed as a fraction of the total VMAT2 immunoreactivity in all peak fractions. Only the two peak LDCV fractions containing ^{35}S-SgII were used to determine the amount of VMAT2 expressed on i- or mLDCVs. The bars indicate the mean ± SEM (n = 3).

crepancy is that the acidic clusters in the two proteins interact with distinct cytosolic sorting machinery.

The cytoplasmic protein PACS-1 is considered to mediate the retrieval of furin from LDCVs. PACS-1 binds to the phosphorylated acidic cluster in furin and appears to promote retrieval to the TGN through an interaction with the clathrin adaptor protein AP-1 (Wan et al., 1998). To determine whether VMAT2 also binds to PACS-1, we produced GST fusion proteins containing the COOH termini of wild-type, AA, DD, and 507* VMAT2, and examined binding to a bacterially expressed domain of PACS-1 known to interact with furin (Wan et al., 1998). We first compared PACS-1 binding to a GST fusion containing the COOH terminus of wild-type VMAT2 that either was or was not phosphorylated in vitro by casein kinase 2. Very similar to furin, PACS-1 binds more strongly to the phosphorylated than the unphosphorylated form of VMAT2 (Fig. 8). In addition, VMAT2 binds PACS-1 with an avidity similar to furin, supporting the parallel between VMAT2 and furin with respect to this interaction. We then compared PACS-1 binding by wild-type, AA, and DD COOH-terminal VMAT2 domains. As anticipated, PACS-1 binds strongly to the COOH terminus of the DD mutant and at very low levels to wild- type VMAT2 and the other mutants (Fig. 8). Thus, PACS-1 binds specifically and preferentially to the phosphorylated acidic cluster in VMAT2.

Discussion

The analysis of serial COOH-terminal truncations shows that an acidic cluster at the distal COOH terminus of VMAT2 influences localization to LDCVs. The sorting motif includes six acidic residues and two serines previously shown to be phosphorylated by casein kinase 2 (Krantz et al., 1997). By both immunofluorescence and gradient fractionation, deletion of these eight residues reduces VMAT2 expression on LDCVs. Phosphorylation of the acidic cluster apparently has a similar effect on steady state localization of the transporter. Replacement of serines in the cluster by aspartate to mimic phosphorylation reduces localization of VMAT2 to LDCVs. In con-

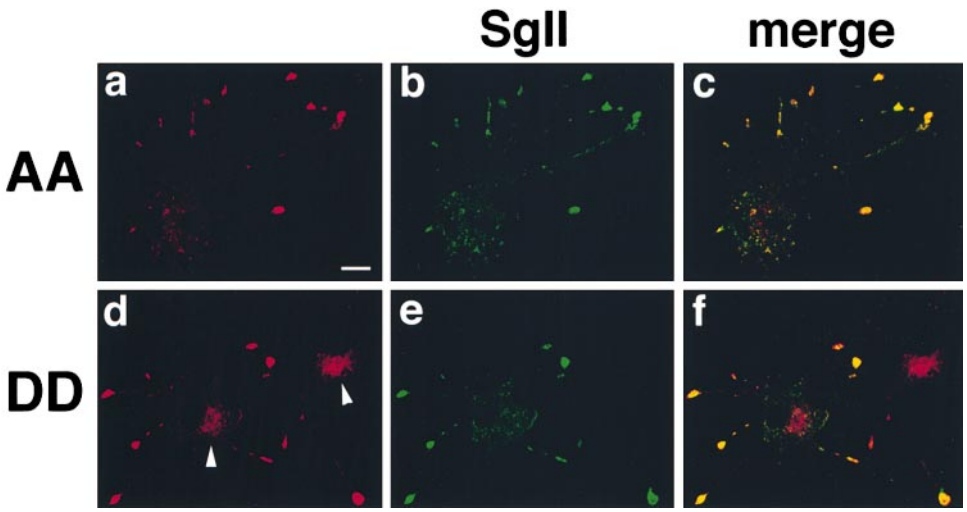

Figure 6. AA and DD VMAT2 differ in the extent of colocalization with SgII. PC12 cells stably expressing AA or DD VMAT2 were double stained for HA using secondary antibodies conjugated to Cy3 (a and d) and for SgII using secondary antibodies conjugated to Cy5 (b and e). The cells were then examined by confocal microscopy. The merged Cy3 and Cy5 images are shown in c and f. The AA mutant colocalizes strongly with SgII, primarily at the tips of cell processes. The DD mutant colocalizes with SgII in the tips of processes, but also exhibits strong perinuclear staining (arrowheads). Bar, 10 μm.

trast, replacement of the serines with alanine to prevent phosphorylation does not perturb the localization of VMAT2 to LDCVs.

Phosphorylation of an acidic cluster in furin reduces LDCV expression by promoting removal during LDCV maturation, and dephosphorylation blocks removal (Jones et al., 1995; Dittie et al., 1997). We now show that the DD mutation reduces VMAT2 expression on m- but not iLDCVs, suggesting that phosphorylation also promotes VMAT2 removal during LDCV maturation. In contrast, the AA mutation that does not permit phosphorylation at these sites does not substantially affect the proportion of VMAT2 on m- versus iLDCVs. Thus, the data strongly suggest that phosphorylation of the acidic cluster reduces the localization of both VMAT2 and furin on LDCVs by promoting their removal during LDCV maturation, whereas dephosphorylation promotes the retention of both proteins on LDCVs.

Although phosphorylation of an acidic cluster appears to promote the removal of both VMAT2 and furin from iLDCVs, VMAT2 normally localizes to LDCVs, whereas furin localizes to the TGN. How can the same motif acting on the same trafficking event contribute to such divergent steady state localization? The acidic clusters in the two proteins may interact with distinct sorting machinery. PACS-1 mediates the retrieval of furin by binding to the phosphorylated acidic cluster (Wan et al., 1998). Removal of VMAT2 from LDCVs may be mediated by a different PACS isoform or an entirely distinct protein interaction. However, we have found that PACS-1 binds to VMAT2 and furin with apparently similar avidity. Further, PACS-1 binds preferentially to the phosphorylated form of the acidic cluster in VMAT2, just as it does with furin.

Since the acidic motifs in VMAT2 and furin have similar effects on subcellular location, influence the same trafficking event, and interact with the same sorting machinery, differences in the state of phosphorylation appear to account for the divergent steady state localization of these two proteins. Phosphorylation by casein kinase 2 is often constitutive; however, dephosphorylation of the acidic cluster in furin has been shown to undergo regulation. Indeed, dephosphorylation by a specific isoform of protein phosphatase 2A regulates the endocytic trafficking of furin (Molloy et al., 1998). Our results now indicate that, just as the persistent phosphorylation of furin in LDCVs promotes its retrieval to the TGN, dephosphorylation of the acidic cluster in VMAT2 appears to promote its retention on mLDCVs.

Previous work has suggested that PACS-1 mediates the retrieval of furin from iLDCVs to the TGN. Consistent with a role for retrieval in the steady state localization of furin to the TGN, reduction of PACS-1 expression redistributes furin out of the TGN (Wan et al., 1998). In addition, PACS-1 links furin to AP-1, a component of the clathrin sorting machinery, and AP-1–dependent retrieval from iLDCVs has been observed for several proteins, including the mannose-6-phosphate receptor (Klumperman et al., 1998). We now show that VMAT2 also binds to PACS-1. However, the 507* mutant undergoes retrieval from LDCVs even though it lacks the acidic cluster and hence cannot interact with PACS-1. Indeed, 507* is excluded from mLDCVs to an even greater extent than the DD mutant, which strongly binds PACS-1. Deletion of the acidic cluster in furin redistributes the protein into endosomes but may not eliminate expression in the TGN (Schafer et al., 1995), suggesting that the motif may not be essential for retrieval from LDCVs. Thus, rather than promoting retrieval, the acidic cluster appears to function as a retention signal that prevents the removal of proteins from LDCVs. Phosphorylation by casein kinase 2 and subsequent binding to PACS-1 presumably inhibit this retention signal and hence promote removal. Conversely, regulated dephosphorylation restores the function of the acidic cluster as a retention signal. Removal from LDCVs may therefore represent a default pathway blocked by the acidic cluster in its dephosphorylated state.

Where do the VMAT2 mutants (507* and DD) go after removal from maturing LDCVs? Although the velocity gradient suggests little expression in the TGN (Fig. 4), the immunofluorescence shows colocalization with TGN38 and to a lesser extent with the late endosomal and lysosomal proteins mannose 6 phosphate receptor and cathepsin B. The mutants may therefore cycle repeatedly between the TGN and iLDCVs, increasing the likelihood of diversion to late endosomes and lysosomes. Supporting this possibility, we have observed increased turnover of 507* ($t_{1/2} \sim 4$ h) relative to wild-type VMAT2 ($t_{1/2} \sim 7$ h). Alternatively, the removal of 507* and DD mutants from maturing LDCVs might increase their trafficking to the constitutive secretory pathway and hence to SLMVs. Immunofluorescence and gradient fractionation indicate

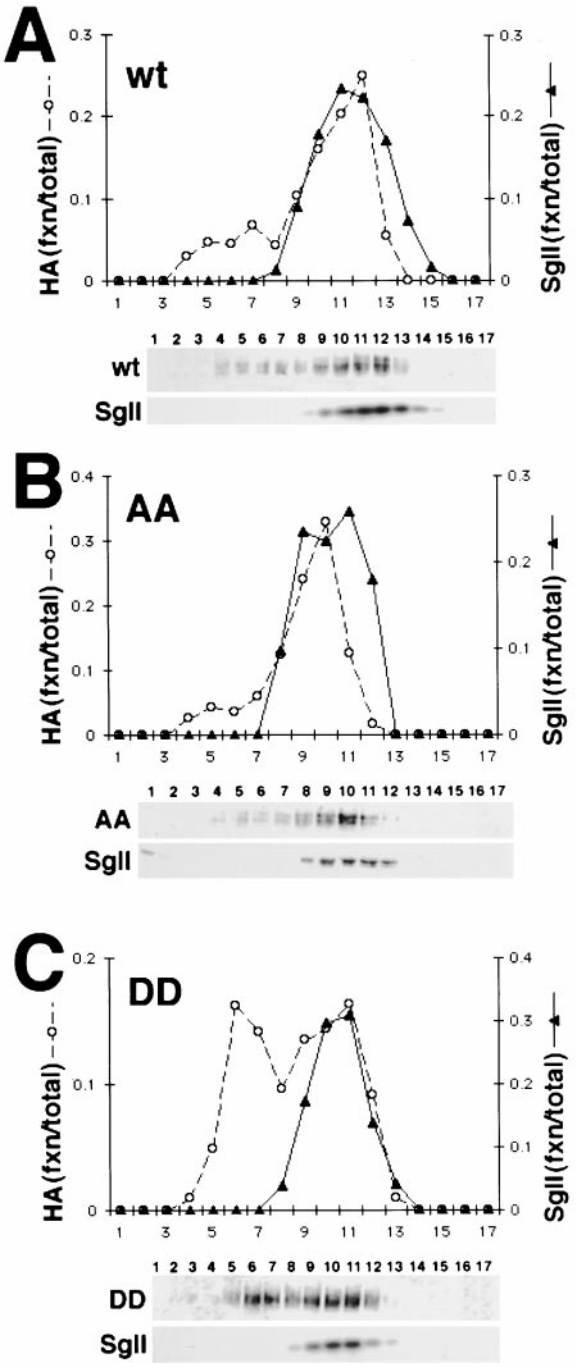

Figure 7. Density gradient fractionation of AA and DD VMAT2. Post-nuclear supernatants from PC12 cells stably expressing HA-tagged wild-type (A), AA (B), and DD (C) VMAT2 were separated by equilibrium gradient centrifugation through 0.6–1.6 M sucrose and the fractions analyzed by Western blotting for HA (A–C, top), and SgII (bottom). The gradients shown were then quantified using NIH Image and the amount of VMAT2 and SgII expressed as a fraction of the total immunoreactivity. Wild-type and AA VMAT2 cofractionate with SgII in heavy fractions. DD also cofractionates with SgII, but has a second peak in lighter fractions. The analysis of three different stable cell lines for each construct yielded similar results.

some colocalization of 507* with synaptophysin (Figs. 3, a–c, and 5 B). However, we have not observed any increased expression of these mutants on SLMVs separated from other membrane vesicles by glycerol velocity gradient

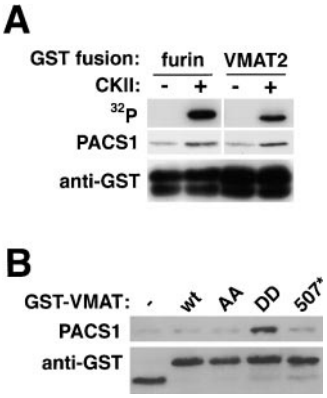

Figure 8. PACS-1 binding to the VMAT2 COOH terminus. (A) GST fusion proteins containing the COOH terminus of wild-type VMAT2 or furin were bound to glutathione-sepharose beads and phosphorylated using casein kinase 2. Unphosphorylated and phosphorylated fusion proteins bound to glutathione-sepharose were then incubated with a poly-His–tagged version of the PACS-1 furin-binding domain and the bound protein detected using an antipolyhistidine antibody (PACS-1). Autoradiography was used to assess protein phosphorylation (^{32}P). Western analysis for GST confirmed the presence of equal amounts of unphosphorylated and phosphorylated GST fusion proteins. Similar to phosphorylated furin, phosphorylated VMAT2 binds PACS-1 more strongly than the unphosphorylated protein. (B) GST fusion proteins containing the COOH termini of wild-type, AA, DD, or 507* VMAT2 were incubated with the furin-binding domain of PACS-1 as described in A. Western analysis was then used as described above to detect bound PACS-1 and confirm the presence of equal amounts of GST fusions. PACS-1 binds strongly to the DD mutant, but poorly to wild-type VMAT2 and the AA mutant.

fractionation (Clift-O'Grady et al., 1990; Krantz, D.E., C. Waites, R.H. Edwards, unpublished observations). In addition, we have not detected the constitutive delivery of 507* and DD mutants to the cell surface (data not shown). In contrast to mutants defective in sorting to the regulated secretory pathway, which internalize large amounts of HA antibody from the medium due to their external HA epitope and their constitutive delivery at the cell surface (Waites, C., and R.H. Edwards, manuscript in preparation), wild-type, 507*, DD, and AA VMAT2 exhibit very little uptake of the HA antibody. Thus, the COOH-terminal acidic cluster appears to have little role in sorting to the regulated secretory pathway in the TGN.

Since acidic residues upstream of the IL motif in VMAT2 also contribute to localization on LDCVs, what is the relationship between these residues and the more COOH-terminal acidic cluster? The two motifs may both be required for retention on LDCVs. However, acidic residues upstream of the dileucine motif in other proteins have been shown to promote internalization from the plasma membrane (Pond et al., 1995; Dietrich et al., 1997), suggesting that these residues would more likely promote than inhibit VMAT2 removal from LDCVs. Alternatively, the two glutamates upstream of the dileucine-like motif may be required for another trafficking event such as sorting in endosomes or the TGN.

VMAT2 sorts to synaptic vesicles and tubulovesicular structures as well as LDCVs (Nirenberg et al., 1995, 1996, 1997), indicating the potential of acidic cluster phosphorylation to regulate the proportion of protein on these different populations of neurosecretory vesicles. Since LDCVs reside in the cell body and dendrites as well as the nerve terminal, alterations in the expression of VMAT2 on LDCVs have the potential to affect somatodendritic release. LDCVs also differ from SVs and other secretory vesicles in their responsiveness to different stimuli, and in the rate of release

(Bruns and Jahn, 1995). The regulation of VMAT2 phosphorylation on its acidic cluster may thus influence the site, mode, and hence the role of monoamines in signaling.

In summary, VMAT2 resembles furin with respect to the influence of phosphorylation on membrane trafficking and on binding to PACS-1, but VMAT2 differs in steady state location. Differences in phosphorylation state apparently confer the differences in subcellular distribution by regulating removal from LDCVs. In addition, the acidic motif in VMAT2 acts as a retention signal that is inactivated by phosphorylation, rather than as a positive signal for removal from LDCVs. The motif may thus interact in its unphosphorylated state with a protein that retains VMAT2 on LDCVs. Phosphorylation may displace this protein, promoting an interaction with PACS and removal from LDCVs. A large number of membrane proteins including the synaptic vesicle protein synaptotagmin as well as furin and VMAT2 contain acidic motifs phosphorylated by casein kinase (Bennett et al., 1993; Molloy et al., 1999). The mechanism of regulated retention may therefore act at multiple trafficking events to influence the subcellular distribution and physiological role of many proteins.

We thank Yongjian Liu for crucial reagents and technical guidance, and Regis Kelly and Mark von Zastrow for helpful suggestions.

This study was supported by grants from the Howard Hughes Medical Institute (to A. Mehta and D.E. Krantz), the National Institute on Drug Abuse (to D.E. Krantz and R.H. Edwards), and the National Institutes of Health (to R.H. Edwards).

Submitted: 10 November 2000
Revised: 26 December 2000
Accepted: 23 January 2001

References

Aghajanian, G.K., and B.S. Bunney. 1974. Pre- and postsynaptic feedback mechanisms in central dopaminergic neurons. *In* Frontiers of Neurology and Neuroscience Research. P. Seeman and G.M. Brown, editors. University of Toronto Press, Toronto, Ontario, Canada. 4–11.

Bennett, M.K., K.G. Miller, and R.H. Scheller. 1993. Casein kinase II phosphorylates the synaptic vesicle protein p65. *J. Neurosci.* 13:1701–1707.

Blagoveshchenskaya, A.D., E.W. Hewitt, and D.F. Cutler. 1999. A complex web of signal-dependent trafficking underlies the triorganellar distribution of P-selectin in neuroendocrine PC12 cells. *J. Cell Biol.* 145:1419–1433.

Bruns, D., and R. Jahn. 1995. Real-time measurement of transmitter release from single synaptic vesicles. *Nature.* 377:62–65.

Calakos, N., and R.H. Scheller. 1996. Synaptic vesicle biogenesis, docking, and fusion: a molecular description. *Physiol. Rev.* 76:1–29.

Cheramy, A., V. Leviel, and J. Glowinski. 1981. Dendritic release of dopamine in the substantia nigra. *Nature.* 289:537–542.

Clift-O'Grady, L., A.D. Linstedt, A.W. Lowe, E. Grote, and R.B. Kelly. 1990. Biogenesis of synaptic vesicle-like structures in a pheochromocytoma cell line PC12. *J. Cell Biol.* 110:1693–1703.

De Camilli, P., and R. Jahn. 1990. Pathways to regulated exocytosis in neurons. *Annu. Rev. Physiol.* 52:625–645.

Dietrich, J., J. Kastrup, B.L. Nielsen, N. Odum, and C. Geisler. 1997. Regulation and function of the CD3 gamma DXXXLL motif: a binding site for adaptor protein-1 and adaptor protein-2 in vitro. *J. Cell Biol.* 138:271–281.

Dittie, A.S., N. Hajibagheri, and S.A. Tooze. 1996. The AP-1 adaptor complex binds to immature secretory granules from PC12 cells, and is regulated by ADP-ribosylation factor. *J. Cell Biol.* 132:523–536.

Dittie, A.S., L. Thomas, G. Thomas, and S.A. Tooze. 1997. Interaction of furin in immature secretory granules from neuroendocrine cells with the AP-1 adaptor complex is modulated by casein kinase II. *EMBO (Eur. Mol. Biol. Organ.) J.* 16:4859–4870.

Geffen, L.B., T.M. Jessel, A.C. Cuello, and L.L. Iverson. 1976. Release of dopamine from dendrites in rat substantia nigra. *Nature.* 260:258–260.

Grace, A.A., and B.S. Bunney. 1995. Electrophysiological properties of midbrain dopamine neurons. *In* Psychopharmacology: The Fourth Generation of Progress. F.E. Bloom and D.J. Kupfer, editors. Raven Press, New York, NY. 163–178.

Heeringa, M.J., and E.D. Abercrombie. 1995. Biochemistry of somatodendritic dopamine release in substantia nigra: an in vivo comparison with striatal dopamine release. *J. Neurochem.* 65:192–200.

Jaffe, E.H., A. Marty, A. Schulte, and R.H. Chow. 1998. Extrasynaptic vesicular transmitter release from the somata of substantia nigra neurons in rat midbrain slices. *J. Neurosci.* 18:3548–3553.

Jones, B.G., L. Thomas, S.S. Molloy, C.D. Thulin, M.D. Fry, K.A. Walsh, and G. Thomas. 1995. Intracellular trafficking of furin is modulated by the phosphorylation state of a casein kinase II site in its cytoplasmic tail. *EMBO (Eur. Mol. Biol. Organ.) J.* 14:5869–5883.

Kelly, R.B., and E. Grote. 1993. Protein targeting in the neuron. *Annu. Rev. Neurosci.* 16:95–127.

Klumperman, J., R. Kuliawat, J.M. Griffith, H.J. Geuze, and P. Arvan. 1998. Mannose-6-phosphate receptors are sorted from immature secretory granules via adaptor protein AP-1, clathrin and syntaxin 6-positive vesicles. *J. Cell Biol.* 141:359–371.

Krantz, D.E., D. Peter, Y. Liu, and R.H. Edwards. 1997. Phosphorylation of a vesicular monoamine transporter by casein kinase II. *J. Biol. Chem.* 272: 6752–6759.

Krantz, D.E., C. Waites, V. Oorschot, Y. Liu, R.I. Wilson, P.K. Tan, J. Klumperman, and R.H. Edwards. 2000. A phosphorylation site regulates sorting of the vesicular acetylcholine transporter to dense core vesicles. *J. Cell Biol.* 149:379–395.

Kuliawat, R., J. Klumperman, T. Ludwig, and P. Arvan. 1997. Differential sorting of lysosomal enzymes out of the regulated secretory pathway in pancreatic beta-cells. *J. Cell Biol.* 137:595–608.

Kunkel, T.A., K. Bebenek, and J. McClary. 1991. Efficient site-directed mutagenesis using uracil-containing DNA. *Methods Enzymol.* 204:125–139.

Liu, Y., and R.H. Edwards. 1997. Differential localization of vesicular acetylcholine and monoamine transporters in PC12 cells but not CHO cells. *J. Cell. Biol.* 139:907–916.

Liu, Y., E.S. Schweitzer, M.J. Nirenberg, V.M. Pickel, C.J. Evans, and R.H. Edwards. 1994. Preferential localization of a vesicular monoamine transporter to dense core vesicles in PC12 cells. *J. Cell Biol.* 127:1419–1433.

Martin, T.F.J. 1994. The molecular machinery for fast and slow neurosecretion. *Curr. Opin. Neurobiol.* 4:626–632.

Molloy, S.S., E.D. Anderson, F. Jean, and G. Thomas. 1999. Bi-cycling the furin pathway: from TGN localization to pathogen activation and embryogenesis. *Trends Cell Biol.* 9:28–35.

Molloy, S.S., L. Thomas, C. Kamibayashi, M.C. Mumby, and G. Thomas. 1998. Regulation of endosome sorting by a specific PP2A isoform. *J. Cell Biol.* 142: 1399–1411.

Molloy, S.S., L. Thomas, J.K. VanSlyke, P.E. Stenberg, and G. Thomas. 1994. Intracellular trafficking and activation of the furin proprotein convertase: localization to the TGN and recycling from the cell surface. *EMBO (Eur. Mol. Biol. Organ.) J.* 13:18–33.

Nirenberg, M.J., J. Chan, Y. Liu, R.H. Edwards, and V.M. Pickel. 1996. Ultrastructural localization of the monoamine transporter-2 in midbrain dopaminergic neurons: potential sites for somatodendritic storage and release of dopamine. *J. Neurosci.* 16:4135–4145.

Nirenberg, M.J., J. Chan, Y. Liu, R.H. Edwards, and V.M. Pickel. 1997. Vesicular monoamine transporter-2: immunogold localization in striatal axons and terminals. *Synapse.* 26:194–198.

Nirenberg, M.J., Y. Liu, D. Peter, R.H. Edwards, and V.M. Pickel. 1995. The vesicular monoamine transporter-2 is present in small synaptic vesicles and preferentially localizes to large dense core vesicles in rat solitary tract nuclei. *Proc. Natl. Acad. Sci. USA.* 92:8773–8777.

Peter, D., Y. Liu, C. Sternini, R. de Giorgio, N. Brecha, and R.H. Edwards. 1995. Differential expression of two vesicular monoamine transporters. *J. Neurosci.* 15:6179–6188.

Pond, L., L.A. Kuhn, L. Teyton, M.-P. Schutze, J.A. Tainer, M.R. Jackson, and P.A. Peterson. 1995. A role for acidic residues in di-leucine motif-based targeting to the endocytic pathway. *J. Biol. Chem.* 270:19989–19997.

Robertson, G.S., G. Damsma, and H.C. Fibiger. 1991. Characterization of dopamine release in the substantia nigra by in vivo microdialysis in freely moving rats. *J. Neurosci.* 11:2209–2216.

Schafer, W., A. Stroh, S. Berghofer, J. Seiler, M. Vey, M.L. Kruse, H.F. Kern, H.D. Klenk, and W. Garten. 1995. Two independent targeting signals in the cytoplasmic domain determine trans-Golgi network localization and endosomal trafficking of the proprotein convertase furin. *EMBO (Eur. Mol. Biol. Organ.) J.* 4:2424–2435.

Sudhof, T.C. 1995. The synaptic vesicle cycle: a cascade of protein–protein interactions. *Nature.* 375:645–653.

Tan, P.K., C. Waites, Y. Liu, D.E. Krantz, and R.H. Edwards. 1998. A leucine-based motif mediates the endocytosis of vesicular monoamine and acetylcholine transporters. *J. Biol. Chem.* 28:17351–17360.

Tooze, S.A., E. Chanat, J. Tooze, and W.B. Huttner. 1993. Secretory granule formation. *In* Mechanisms of intracellular trafficking and processing of proproteins. CRC Press, Boca Raton, FL. 157–177.

Tooze, S.A., and W.B. Huttner. 1990. Cell-free protein sorting to the regulated and constitutive secretory pathways. *Cell.* 60:837–847.

Varoqui, H., and J.D. Erickson. 1998. The cytoplasmic tail of the vesicular acetylcholine transporter contains a synaptic vesicle targeting signal. *J. Biol. Chem.* 273:9094–9098.

Wan, L., S.S. Molloy, L. Thomas, G. Liu, Y. Xiang, S.L. Rybak, and G. Thomas. 1998. PACS-1 defines a novel gene family of cytosolic sorting proteins required for trans-Golgi network localization. *Cell.* 94:205–216.

Weihe, E., M.K. Schäfer, J.D. Erickson, and L.E. Eiden. 1994. Localization of vesicular monoamine transporter isoforms (VMAT1 and VMAT2) to endocrine cells and neurons in rat. *J. Mol.Neurosci.* 5:149–164.

Xiang, Y., S.S. Molloy, L. Thomas, and G. Thomas. 2000. The PC6B cytoplasmic domain contains two acidic clusters that direct sorting to distinct trans-Golgi network/endosomal compartments. *Mol. Biol. Cell.* 11:1257–1273.